Neuron, Vol. 23, 659–674, August, 1999, Copyright ©1999 by Cell Press

Requirement for the Homeobox Gene *Hb9* in the Consolidation of Motor Neuron Identity

Silvia Arber,† Barbara Han, Monica Mendelsohn, Michael Smith, Thomas M. Jessell,* and Shanthini Sockanathan†
Howard Hughes Medical Institute
Department of Biochemistry
and Molecular Biophysics
Center for Neurobiology and Behavior
Columbia University
New York, New York 10032

Summary

The homeobox gene *Hb9*, like its close relative *MNR2*, is expressed selectively by motor neurons (MNs) in the developing vertebrate CNS. In embryonic chick spinal cord, the ectopic expression of *MNR2* or *Hb9* is sufficient to trigger MN differentiation and to repress the differentiation of an adjacent population of V2 interneurons. Here, we provide genetic evidence that *Hb9* has an essential role in MN differentiation. In mice lacking *Hb9* function, MNs are generated on schedule and in normal numbers but transiently acquire molecular features of V2 interneurons. The aberrant specification of MN identity is associated with defects in the migration of MNs, the emergence of the subtype identities of MNs, and the projection of motor axons. These findings show that HB9 has an essential function in consolidating the identity of postmitotic MNs.

Introduction

The ability of neurons to form selective neuronal circuits is a function of the molecular properties that they acquire at early stages of their differentiation. The molecular features that distinguish individual classes of neurons appear to control the pattern of axonal projections, the formation of target connections, and the expression of specific chemical transmitters. The emergence of a coherent neuronal phenotype is a protracted process and is thought to involve progressive restrictions in the developmental potential of both neural progenitor cells and postmitotic neurons (Cepko, 1999; Edlund and Jessell, 1999). In the peripheral nervous system, convergent programs of transcription factor expression have been suggested to coordinate panneuronal properties with more specific aspects of neuronal subtype identity, notably, neurotransmitter synthesis and trophic factor sensitivity (Lo et al., 1998, 1999; Goridis and Brunet, 1999; Pattyn et al., 1999).

When and how neuronal subclasses in the CNS acquire their specialized functional properties is less well understood. Studies of the differentiation of spinal motor neurons (MNs) have provided some insight into the steps that confer neuronal subtype identity within the CNS. Physiological and anatomical studies have revealed that spinal MNs exhibit several levels of organization and function (Landmesser, 1978a, 1978b), and these have a molecular correlate in the selective patterns of expression of different families of transcription factors (Tanabe and Jessell, 1996; Goulding, 1998). Members of the LIM homeodomain (LIM-HD) protein family define aspects of the generic and columnar identities of spinal MNs (Ericson et al., 1992, 1996; Tsuchida et al., 1994; Sharma et al., 1998). In addition, many of the MN pools that innervate individual muscles in the limb can be defined by the expression of ETS domain proteins (Lin et al., 1998). The analysis of neuronal fate changes that result from the misexpression or inactivation of certain of these nuclear factors has lent support to the idea that they have critical roles in the specification of MN identity (Sharma et al., 1998; Tanabe et al., 1998; see Appel, 1999).

Some of the earlier events that specify the differentiation of neural progenitors into MNs have also been defined. The differentiation of MNs is initiated when progenitor cells located in the ventral half of the neural tube acquire distinct identities in response to the graded signaling activity of Sonic hedgehog (Shh) (Ericson et al., 1996, 1997a, 1997b; Briscoe et al., 1999). The final division of MN progenitors in chick is marked by the onset of expression of two homeodomain proteins, MNR2 and Lim3 (Lhx3), which appear to have distinct roles in MN differentiation (Ericson et al., 1997a; Sharma et al., 1998; Tanabe et al., 1998). MNR2 expression is restricted to MN progenitors, whereas Lim3 is expressed by progenitor cells that give rise to an adjacent population of V2 interneurons (Ericson et al., 1997a; Tanabe et al., 1998). In chick, the ectopic expression of MNR2 is sufficient to direct the differentiation of neural cells into MNs and to suppress V2 interneuron generation (Tanabe et al., 1998). In contrast, ectopic expression of Lim3 alone appears to promote the generation of V2 interneurons (Tanabe et al., 1998). These results suggest that MNR2 has a role in specifying whether ventral progenitors that express Lim3 generate MNs rather than V2 neurons.

The function of many of the other transcription factors whose expression is restricted to MNs has not yet been addressed. Among these, the homeobox gene *Hb9* (Harrison et al., 1994; Ross et al., 1998) is a selective marker of MNs in the developing spinal cord (Pfaff et al., 1996; Saha et al., 1997; Tanabe et al., 1998). Strikingly, HB9 possesses a homeodomain virtually identical to that of MNR2. Moreover, the ectopic expression of HB9 in chick has been shown to mimic the MN-inducing and V2 interneuron–repressive activities of MNR2 (Tanabe et al., unpublished data). In contrast to MNR2, however, the expression of HB9 in chick is excluded from ventral progenitor cells and is restricted to postmitotic MNs (Tanabe et al., 1998), suggesting that it has a later role in the differentiation of postmitotic MNs. Further insight into the developmental roles of MNR2 and HB9, however, requires an analysis of MN differentiation in embryos that lack the function of these homeodomain proteins.

To begin to address this issue, we have examined MN

*To whom correspondence should be addressed (e-mail: tmj1@columbia.edu).
† These authors contributed equally to this work.

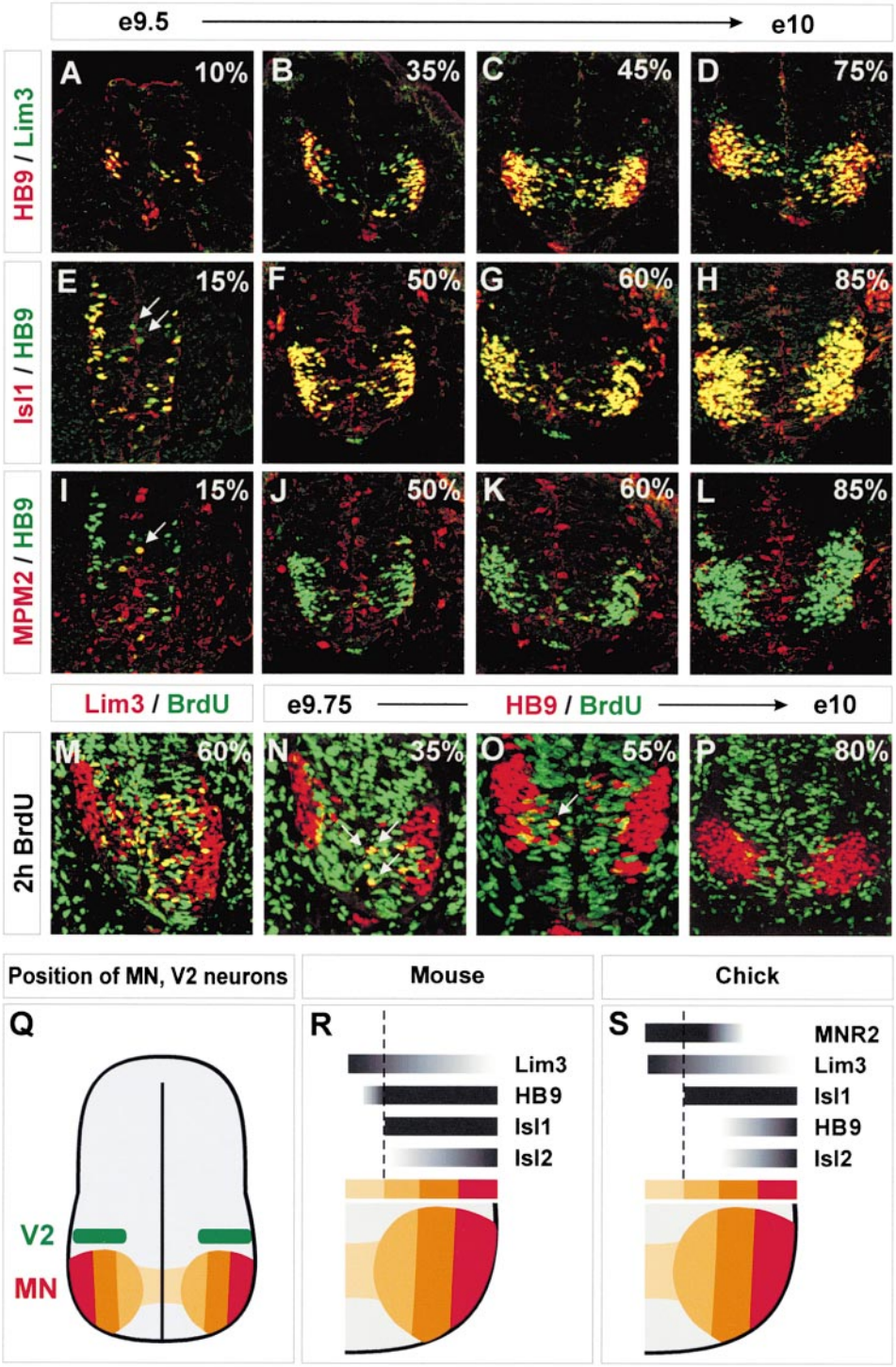

Figure 1. Early Expression of HB9 by Developing MNs

(A–D) Comparison of the expression of HB9 (red) and Lim3 (Lhx3) (green) in developing MNs at the caudal cervical levels of E9.5–E10 mouse embryos. Percentages in each panel indicate the approximate fraction of MNs detected at the time of analysis compared with the total number of MNs generated by E11 (see Figure 3A).

(A) At ~E9.5 (10%–25% MN generation), HB9 and Lim3 are coexpressed by most labeled cells although occasional $Lim3^{+}/HB9^{-}$ cells are detected.

(B and C) At slightly older ages (~E9.75, 30%–60% MN generation), many medially located $Lim3^{+}/HB9^{-}$ cells are detected, and most double-labeled cells are confined to the lateral margins of the ventral spinal cord.

(D) A similar profile is observed near the end of the period of MN generation. The notochord is also labeled at these developmental stages.

(E–H) Comparison of expression of HB9 (red) and Isl1 (green) in developing MNs located at the caudal cervical levels of E9.5–E10 mouse embryos.

development in mice in which the *Hb9* gene has been inactivated by targeted mutation. In mice lacking *Hb9* function, MNs are generated on schedule and in normal numbers. However, soon after MNs have left the cell cycle, there is a dramatic change in the program of MN differentiation. Most strikingly, MNs transiently express transcription factors normally characteristic of V2 interneurons. In addition, and perhaps as a consequence, the transcription factor codes that define the columnar and pool identities of spinal MNs are markedly disrupted. These defects in the transcription factor profile of MNs are accompanied by abnormal MN migratory patterns, errors in motor axon projections, and defects in the innervation of certain target muscles. Together, these results provide evidence that HB9 has a critical role in the consolidation of MN identity, in particular, in repressing the expression of V2 interneuron character.

Results

HB9 Expression in Developing MNs

To begin to define the role of HB9 in the early development of MNs, we compared the pattern of HB9 expression with that of three other early MN markers, the LIM-HD proteins Lim3 (Lhx3), Isl1, and Isl2. In the mouse spinal cord and caudal hindbrain, the first postmitotic MNs are detected at E9–E9.5, and MN genesis is complete by E10.5–E11 (Nornes and Carry, 1978; Figure 3A; our unpublished data). Expression of HB9 was first detected in the spinal cord at E9.25–E9.5 (Figure 1; data not shown). During the early phase of MN generation (when ~10%–25% of the total number of MNs destined to form at a specific axial level have been generated), the expression of HB9 was largely coincident with that of Lim3 (Figure 1A; data not shown), and $HB9^+/Lim3^+$ cells that lacked Isl1 expression could also be detected (Figure 1E). However, during the peak period of MN generation (25%–60% of total MN number), many medially located $Lim3^+$ cells lacked HB9 expression (Figures 1B–1D), and the expression of HB9 and Isl1 coincided in virtually all cells (Figures 1F–1H). At ~E10, near to the completion of the period of MN generation (60%–85% MN genesis), HB9 and Isl1 expression also coincided, but by this stage, many of the more lateral and thus more mature HB9 cells had lost Lim3 expression (see Figures 4A and 4E). Within the developing spinal cord, HB9 expression was detected in all MNs, regardless of their eventual somatic or visceral subclass identity (data not shown). However, a more selective profile of HB9 expression was detected at caudal hindbrain levels. Here, HB9 expression was restricted to somatic MNs of the hypoglossal nucleus, and no expression was detected in cranial level MNs of visceral identity (data not shown, but see Briscoe et al., 1999). Notochord cells also transiently expressed HB9, from E8.5–E9.5 (Figures 1A–1D; data not shown).

Comparison of the patterns of expression of Lim3, HB9, and Isl1 raised the issue of the relationship between the time of onset of HB9 expression and the exit of MNs from the cell cycle. To assess this issue, we determined over the period E9.5–E10 the incidence of overlap in expression of HB9 with MPM2, a marker of M phase cells (Westendorf et al., 1994), and with cells labeled by a brief bromodeoxyuridine (BrdU) pulse. The incidence of coexpression of MPM2 and HB9 by individual cells varied markedly according to the fraction of the total number of MNs generated at particular axial levels of the spinal cord. We focused our quantitative analysis of HB9 and MPM2 expression at caudal cervical levels of the spinal cord. The incidence of MPM2/HB9 coexpression was greatest in younger (~E9.5) embryos in which only 10%–25% of the total number of MNs had been generated (Figure 1I; data not shown). In slightly older (~E9.75) embryos, when MN generation was approaching its peak (25%–60% of MNs generated), very few MPM2/HB9-colabeled cells were detected (Figures 1J–1L). During the later phase (~E10) of MN generation (>60% MNs generated), few if any HB9 cells coexpressed MPM2 (Figure 1L). BrdU labeling analysis of E9.5–E10 embryos revealed that at early stages of MN genesis, $BrdU^+/HB9^+$ cells could be detected (Figure 1N), but during the peak and late periods of MN genesis, the number of $BrdU^+/HB9^+$ cells decreased markedly (Figures 1O and 1P). In contrast, many $BrdU^+/Lim3^+$ cells were detected in the ventral domain of MN generation throughout the entire period of MN genesis (Figure 1M; data not shown). These data indicate that HB9 is expressed by some $Lim3^+$ MN progenitors during the

(E) In ~E9.5 embryos (10%–15% MN generation), HB9 and Isl1 are coexpressed by most cells although occasional $HB9^+/Isl1^-$ cells are detected (arrows).

(F and G) At slightly older stages (E9.75, 50%–60% MN generation) HB9 and Isl1 are coexpressed by virtually all cells in the ventral spinal cord. Note the expression of Isl1 but not of HB9 in sensory neurons in the DRGs in (G). A similar profile is observed near the completion (85%) of MN generation (H).

(I–L) Comparison of HB9 and MPM2 expression in developing MNs located at the caudal cervical levels of E9.5–E10 mouse embryos.

(I) In ~E9.5 embryos (10%–15% MN generation), ~10% of medially located $MPM2^+$ cells express HB9 (arrow) although many ventral $MPM2^+$ cells within the domain of MN generation lack HB9 expression.

(J and K) At slightly older stages (~E9.75, 25%–60% MN generation) only 3% of MPM2 cells express HB9. Near the completion of MN generation (>60% MN generation), no $MPM2^+$ cells coexpressed HB9, although many $MPM2^+/Lim3^+$ cells were detected (data not shown). MPM2 analysis was based on at least six embryos examined over the period E9.5–E10.

(M) BrdU expression in many $Lim3^+$ cells in the ventral domain of MN generation, assayed during the peak period (60%) of MN genesis.

(N–P) Sections through E9.75 and E10 embryos pulse labeled with BrdU in vivo for 2 hr. At early stages of MN genesis, a few $BrdU^+/HB9^+$ cells are detected (N), but during the peak (O) and late (P) periods of MN genesis, the number of $BrdU^+/HB9^+$ cells drops dramatically. BrdU analysis was performed in at least six embryos.

(Q) The position of generation of MNs and V2 interneurons.

(R and S) Diagrams indicating the temporal profile of expression of HB9 in the early differentiation of mouse (R) and chick (S) spinal MNs, assessed by expression of homeodomain transcription factors. The sequential stages in the conversion of MN progenitors into postmitotic MNs in chick are based on the data of Tanabe et al. (1998). Dashed vertical line indicates approximate time of cell cycle exit.

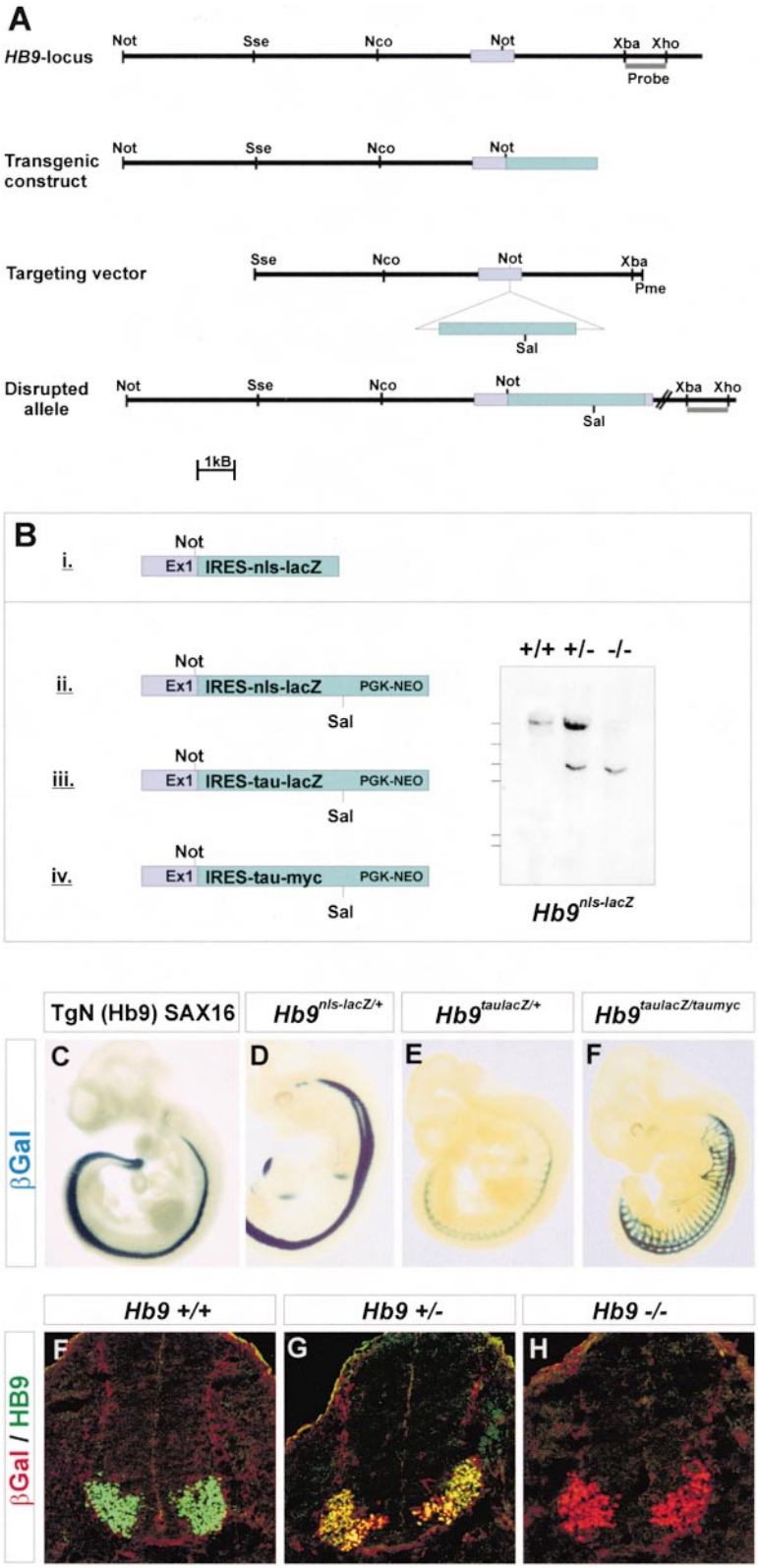

Figure 2. Inactivation of *Hb9* by Homologous Recombination

(A) Diagrams show strategy for homologous recombination, at the *Hb9* locus in ES cells, for generating a disrupted allele of *Hb9* and the transgenic construct used to define an MN regulatory region in the *Hb9* locus. A 9 kb NotI fragment comprising the 5′ upstream region of the *Hb9* gene and sequence from the first exon (blue) of *Hb9* was used to generate a transgenic construct. To generate a disrupted *Hb9* allele, targeting cassettes were integrated into the NotI site of the first of three exons of the *Hb9* gene (data not shown). A 6 kB 5′ region (Sse83871–NotI) and a 3 kB 3′ region (NotI–XbaI) were used to generate the basic targeting vector into which the targeting cassettes (green) were integrated. The probe to screen ES cells for the detection of homologous recombination was a 1 kB XbaI–XhoI (shaded bar) fragment located 3′ to the region used for the generation of the targeting construct.

(B) Targeting cassettes used for the generation of transgenic mice (IRES-*nlslacZ* [i]) and *Hb9* alleles by homologous recombination in ES cells (IRES-*nlslacZ* [ii], IRES-*taulacZ* [ii], and IRES-*taumyc* [iv]). For homologous recombination, a *pgk-neo* cassette flanked by loxP sites was inserted 3′ to a SalI site.

(Right) Representative Southern blot of $Hb9^{nlslacZ}$ genomic DNA derived from $Hb9^{+/+}$, $Hb9^{nlslacZ/+}$, and $Hb9^{nlslacZ/nlslacZ}$ embryos (6 kB mutant band, 20 kB wild-type band; lines to the left indicate molecular weight standards; SalI/XhoI digest). Similar diagnostic blots were obtained from the other two targeted alleles (available on request).

(C–F) Analysis of whole-mount embryos stained for β-gal activity.

(C) E10 transgenic embryo (TgN(*Hb9*)SAX16) labeled for β-gal expression.

(D) E11.5 $Hb9^{nlslacZ/+}$ embryo. The staining in the developing limbs corresponds to the region of the zone of polarizing activity (zpa).

(E and F) β-gal staining of E11.5 $Hb9^{taulacZ/+}$ (E) and compound mutant $Hb9^{taulacZ/taumyc}$ (F) embryos. In the presence of one allele of *taulacZ*, the staining intensity in the compound homozygote is ~5-fold higher than in the heterozygote. Embryos were processed for the same incubation time.

(F) Expression of HB9 in the spinal cord of E10.5 wild-type embryos.

(G) Coincidence of expression of HB9 protein (green) and nlsLacZ (β-gal) (red) in E10.5 $Hb9^{nlslacZ/+}$ spinal cord.

(H) Absence of HB9 protein in the spinal cord of E10.5 $Hb9^{nlslacZ/nlslacZ}$ embryos.

early phase of MN genesis but also suggest that during the peak period of MN genesis, many cells initiate HB9 expression after the onset of Lim3 expression and coincident with the onset of Isl1 expression, apparently as they acquire a postmitotic state.

Generation of *Hb9* Mutant Mice

To examine the role of *Hb9* in early MN development, we generated targeted alleles of *Hb9* by homologous recombination in mouse embryonic stem (ES) cells. Three *Hb9* alleles were generated, each containing a

Table 1. Generation of *Hb9* Mutant Embryos

	Number of Litters	Number of Embryos	Genotype		
			+/+	+/−	−/−
$Hb9^{nlslacZ}$	14	88	27	40	21
$Hb9^{taumyc}$	6	44	12	22	10
$Hb9^{taulacZ}$	6	41	9	22	10
Total	26	173	48	84	41

pgk-neo gene and cDNAs encoding different marker proteins under the control of an internal ribosome entry site (IRES) sequence (Ghattas et al., 1991; Mombaerts et al., 1996; Figures 2A and 2Bii–2Biv): (1) an SV40 nuclear localization signal (*nls*) fusion with *lacZ* ($Hb9^{nlslacZ}$) (Figure 2D), (2) a *tau* fusion with *lacZ* ($Hb9^{taulacZ}$) (Figures 2E and 2F), and (3) a *tau* fusion with a multimerized *myc* epitope ($Hb9^{taumyc}$) (Figure 5K; data not shown). Mice homozygous for each of the targeted alleles were born at normal Mendelian frequencies (Table 1) but died at or soon after birth (data not shown). The cause of death has not been defined but may involve respiratory failure since the lungs of *Hb9* mutant neonates were not inflated (data not shown).

To determine whether the targeted *Hb9* alleles represented null mutations, we examined the expression of HB9 in heterozygous and homozygous mutant embryos at E10.5. In the spinal cord of heterozygous $Hb9^{nlslacZ}$ embryos, the expression of LacZ and HB9 coincided (Figures 2F and 2G). In mice homozygous for the $Hb9^{nlslacZ}$ allele, the number and position of LacZ cells were similar to those in heterozygotes, but no expression of endogenous HB9 was detected with either N- or C-terminally directed antisera (Figures 2G and 2H; data not shown). Similar results were found in homozygous $Hb9^{taulacZ}$ and $Hb9^{taumyc}$ mutants (data not shown). These results indicate that the targeted *Hb9* alleles represent null mutations and also that the integration of *lacZ* into the *Hb9* locus does not perturb the pattern of gene expression. The spatial pattern of endogenous HB9 expression was also mimicked in transgenic mouse embryos that expressed β-*galactosidase* (β-*gal*; *lacZ*) under the control of a ~9 kb 5′ fragment of the mouse *Hb9* gene (Figures 2A, 2Bi, and 2C; data not shown; see Experimental Procedures).

The persistence of LacZ expression in $Hb9^{nlslacZ}$ mutants indicates that the maintained expression of *Hb9* does not require positive autoregulation. We noted, however, that the level of LacZ expression was much greater in homozygous than in heterozygous $Hb9^{nlslacZ}$ embryos (data not shown). To test whether this increase results from a function of HB9 in the repression of its own expression, we compared the level of LacZ expression in $Hb9^{taulacZ}/Hb9^{taumyc}$ mutant embryos with that in $Hb9^{taulacZ}$ heterozygous embryos. The level of LacZ expression was >5-fold greater in the compound mutants than in $Hb9^{taulacZ}$ heterozygotes (Figures 2E and 2F), even though both sets of embryos expressed only a single $Hb9^{lacZ}$ allele. This result indicates that HB9 represses, directly or indirectly, its own transcription.

MNs Are Generated in Normal Numbers in *Hb9* Mutant Mice

The transient expression of HB9 by the notochord led us to examine whether the loss of *Hb9* function affects the establishment of progenitor cell domains within the ventral neural tube. At E10.5, the expression of Shh, Pax6, and Nkx2.2 in the ventral spinal cord and hindbrain of homozygous $Hb9^{nlslacZ}$ embryos was indistinguishable from that in heterozygous or wild-type littermates (data not shown). Thus, Shh signaling and the establishment of appropriate ventral progenitor cell domains appear to be unaffected in *Hb9* mutants.

We next examined whether the initial generation of postmitotic MNs is affected by the loss of *Hb9* function. LacZ expression was detected in the nuclei of cells in the ventral spinal cord in homozygous $Hb9^{nlslacZ}$ embryos at a position and number identical to those in heterozygotes (Figures 2G, 2H, and 3A). The expression of LacZ persisted in MNs throughout embryonic development in both heterozygous and homozygous $Hb9^{nlslacZ}$ mutant embryos (Figures 3E and 3F; data not shown). Thus, cells in *Hb9* mutant embryos retain an MN identity, as assessed by the transcription of *Hb9* itself. In addition, the total number of Isl1 MNs generated between E9.5 and E10.5 was similar in heterozygous and homozygous $Hb9^{nlslacZ}$ embryos (Figure 4E–4G; data not shown). Moreover, the expression of *Choline Acetyltransferase* (*ChAT*) by MNs persisted in homozygous $Hb9^{nlslacZ}$ embryos (see Figures 6B and 6C; data not shown). Together, these results indicate that HB9 is not required for the initial specification of MN identity.

Defects in MN Migration in *Hb9* Mutant Embryos

To determine whether aspects of the differentiation of postmitotic MNs are affected by the loss of *Hb9* function, we first examined whether the overall spatial organization of MNs within the spinal cord and caudal hindbrain was affected. A marked defect in the pattern of MN migration was detected in *Hb9* mutants. In wild-type and heterozygous $Hb9^{nlslacZ}$ embryos examined at e10–e11, all MN cell bodies are confined to the spinal cord (Figures 2D, 2F, and 2G; data not shown). In contrast, in homozygous $Hb9^{nlslacZ}$ embryos, ~5% of LacZ neurons were detected outside the spinal cord, within the ventral roots (Figure 3B). These extraspinal LacZ neurons, like their counterparts within the spinal cord, coexpressed Isl1 and Isl2 (Figure 3C; data not shown). HB9 is one of the few transcription factors that distinguishes MNs from dorsal root ganglion (DRG) neurons, raising the possibility that the detection of extraspinal LacZ neurons in *Hb9* mutants was a result of their conversion to a DRG neuron identity. However, ectopic LacZ neurons did not express the sensory neuron–specific POU domain protein Brn3.0 (Figure 3D), arguing against their sensory neuron character. These findings reveal a role for HB9 in confining the cell bodies of MNs to the spinal cord.

The settling pattern of the MNs that remained within the spinal cord and caudal hindbrain was also disrupted in *Hb9* mutants. At caudal hindbrain levels in heterozygous $Hb9^{nlslacZ}$ embryos, somatic hypoglossal MNs form a well-delineated nucleus (Figure 3E). Similarly, at cervical and lumbar levels of the spinal cord, a clear separation of median motor column (MMC) MNs and lateral motor column (LMC) MNs is normally evident (Figures 3G and 3I). In contrast, in homozygous $Hb9^{nlslacZ}$ mutants, there was a marked dispersion of MNs in the region of the hypoglossal motor nucleus (Figure 3F), and no clear separation of MMC and LMC neurons was evident at

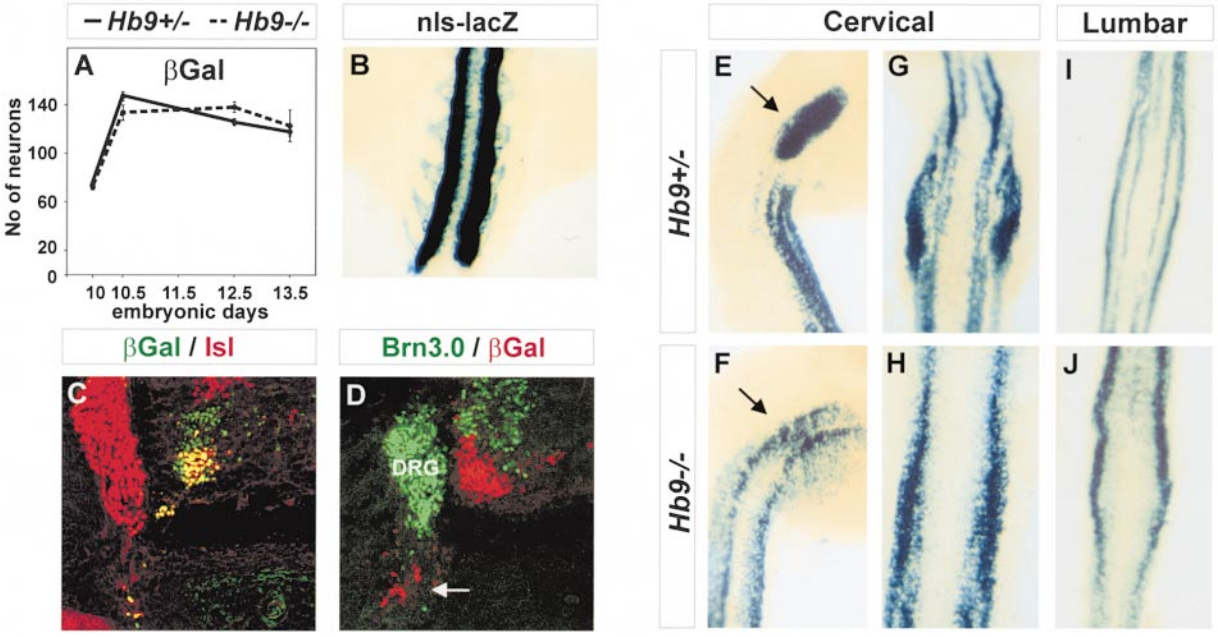

Figure 3. Cell Migration Defects in *Hb9* Mutant Embryos

(A) Analysis of the number of β-gal-labeled cells in brachial spinal cord (cervical 7/8 [C7/8]) at different developmental stages (E10, E10.5, E12.5, and E13.5) in $Hb9^{nlslacZ/+}$ (solid line) and $Hb9^{nlslacZ/nlslacZ}$ (dashed line) embryos.

(B–D) β-gal-labeled neurons in $Hb9^{nlslacZ/nlslacZ}$ embryos are located adjacent to the spinal cord within ventral roots.

(B) Whole-mount β-gal staining of E10.5 lumbar spinal cord showing extraspinal β-gal neurons.

(C) Extraspinal β-gal neurons (green) in an E12.5 embryo coexpress Isl1/2 (red).

(D) Extraspinal β-gal cells (red) in an E12.5 embryo (arrow) do not express the sensory neuron marker Brn3.0. The position of the DRG is shown.

(E–J) Organization of β-gal-labeled cells in the CNS, visualized in whole-mount preparations of E17.5 $Hb9^{nlslacZ/+}$ (E, G, and I) and $Hb9^{nlslacZ/nlslacZ}$ (F, H, and J) embryos.

(E and F) Lateral view of caudal hindbrain and cervical level spinal cord. Arrows point to rostrocaudal level of hypoglossal MNs. Note the clustering of the β-gal-labeled cells in the hypoglossal nucleus in heterozygous embryos but the scattered organization of β-gal-labeled cells along both the dorsoventral and rostrocaudal axes of homozygous $Hb9^{nlslacZ}$ embryos.

(G and H) Ventral view of forelimb-level spinal cord. Note the clear segregation of the MMC (medial strip of β-gal-labeled cells) and LMC (lateral group of β-gal-labeled cells) in the spinal cord of heterozygous $Hb9^{nlslacZ}$ embryos (G) and the extensive intermixing of β-gal-labeled cells in homozygous $Hb9^{nlslacZ}$ embryos (H).

(I and J) Ventral view of lumbar level spinal cord. A clear segregation of β-gal-labeled cells in MMC (medial strip) and LMC (lateral strip) is observed in the spinal cord of heterozygous $Hb9^{nlslacZ}$ embryos (I) but not in homozygous $Hb9^{nlslacZ}$ embryos (J). Similar observations were made in younger stage embryos (E14.5–E16.5).

cervical and lumbar levels (Figures 3H and 3J). These results suggest that the migratory and settling patterns of MNs that underlie the formation of discrete somatic motor nuclei at cranial levels, and of the major somatic motor columns at spinal levels, are disrupted in *Hb9* mutants.

Persistent Expression of Lim3 and Gsh4 by MNs in *Hb9* Mutants

In wild-type embryos, the expression of the LIM-HD proteins Lim3 and Gsh4 is rapidly lost from most postmitotic MNs (Tsuchida et al., 1994; Ericson et al., 1997b; Sharma et al., 1998). To begin to address whether there are changes in the identity of MNs in *Hb9* mutant mice, we examined the profile of expression of Lim3 and Gsh4.

At E10.5, the total number of Lim3 cells was increased ~2-fold in homozygous $Hb9^{nlslacZ}$ embryos compared with heterozygous embryos (Figures 4A–4F). Over 98% of LacZ cells in homozygous $Hb9^{nlslacZ}$ embryos coexpressed Lim3 compared with 23% in heterozygous embryos (Figures 4A, 4B, and 4D), indicating that the increase in Lim3 neurons results from persistent expression in MNs. The persistence of Lim3 expression was widespead, occurring in postmitotic MNs at all spinal levels and in the hypoglossal motor nucleus at caudal hindbrain levels (data not shown). In contrast, the number and position of Lim3 progenitor cells (defined as medial $Lim3^{+}/LacZ^{-}/Isl1^{-}$ cells) was unaffected (Figures 4A and 4B; data not shown). The expression of Gsh4 by MNs was maintained in a manner similar to that of Lim3 (data not shown). These results reveal that HB9 is required for the rapid extinction of Lim3 and Gsh4 expression from most somatic MNs, soon after their exit from the cell cycle. However, the deregulated expression of Lim3 and Gsh4 by MNs in *Hb9* mutant embryos was not sustained. By E12.5–E13.5, the number of Lim3 cells in homozygous $Hb9^{nlslacZ}$ embryos was only 10%–15% greater than that in heterozygous embryos (Figures 4C and 4H), and there was a corresponding decrease in the number of cells that coexpressed Lim3 and LacZ (Figure 4D). Thus, factors other than HB9 are eventually

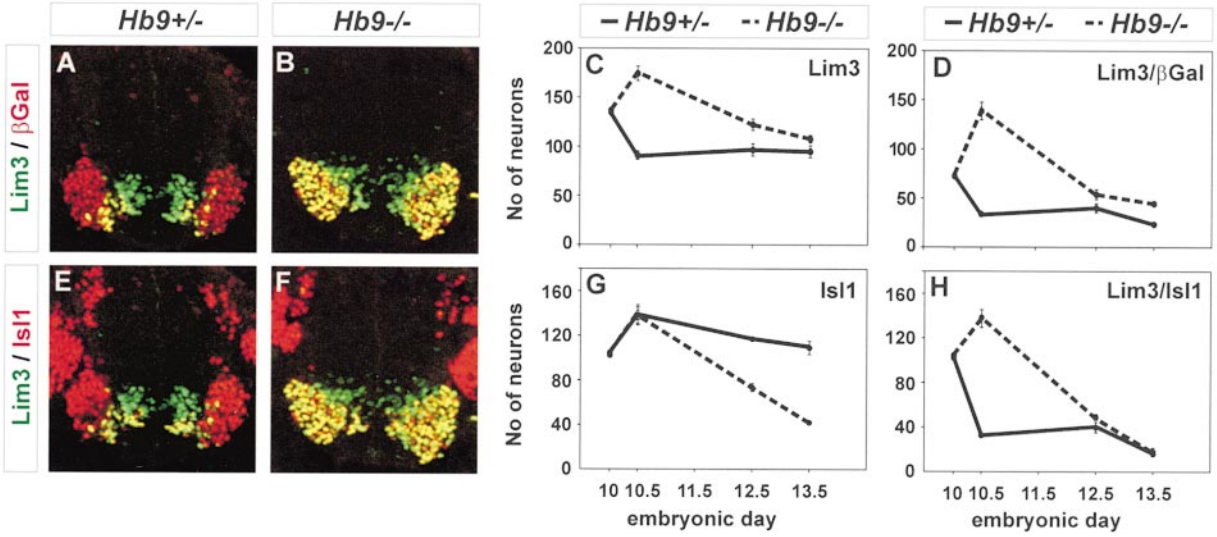

Figure 4. Transient Deregulation of Lim3 in MNs in Mice Lacking *Hb9*

Analysis of Lim3 and Isl1 expression in β-gal-labeled MNs in brachial spinal cord (level C7/8) at different developmental stages in $Hb9^{nlslacZ/+}$ and $Hb9^{nlslacZ/nlslacZ}$ embryos.

(A, B, E, and F) Triple label immunocytochemical detection of Lim3 (green), β-gal (red, [A and B]) and Isl1 (red, [E and F]) on the same sections (A and E, and B and F) of E10.5 $Hb9^{nlslacZ/+}$ and $Hb9^{nlslacZ/nlslacZ}$ embryos. In $Hb9^{nlslacZ/+}$ embryos, MMC MNs maintain Lim3 expression, but most MNs rapidly downregulate Lim3. In $Hb9^{nlslacZ/nlslacZ}$ embryos examined at this stage, virtually all Isl1/β-gal cells coexpress Lim3.

(C, D, G, and H) Developmental time course of Lim3 and Isl1 expression in $Hb9^{nlslacZ/+}$ (solid lines) and $Hb9^{nlslacZ/nlslacZ}$ (dashed lines) embryos.

(C) Number of Lim3 cells.

(D) Number of Lim3/β-gal cells.

(G) Number of Isl1 cells.

(H) Number of Lim3/Isl1 cells. Data from at least three independent sets of experiments for each developmental stage (E10, E10.5, E12.5, and E13.5) are shown. For each stage, the number of positive cells per ventral quadrant of the spinal cord was counted on at least four consecutive sections.

sufficient to extinguish Lim3 and Gsh4 expression from most somatic MNs.

MNs Transiently Acquire V2 Interneuron Character in the Absence of *Hb9* Function

What is the consequence of the persistent expression of Lim3 and Gsh4 by MNs? In wild-type embryos, Lim3 progenitors give rise to both MNs and V2 interneurons (Ericson et al., 1997a), but V2 neurons can be distinguished by the expression of the homeodomain protein Chx10 (Liu et al., 1994; Ericson et al., 1997a). Since Lim3 is sufficient to induce ectopic Chx10 expression in spinal interneurons (Tanabe et al., 1998), we reasoned that the persistence of Lim3 expression in homozygous $Hb9^{nlslacZ}$ embryos might lead MNs to acquire properties characteristic of V2 interneurons. To test this, we examined the expression of Chx10 in homozygous $Hb9^{nlslacZ}$ embryos.

The total number of Chx10 neurons was increased 2- to 3-fold in homozygous $Hb9^{nlslacZ}$ embryos examined over the period E10.5–E12.5 (Figures 5A–5F). To determine whether the increase in Chx10 neurons reflects expression in MNs, we examined the incidence of coexpression of Chx10 and LacZ. No coexpression of Chx10 and LacZ was detected in heterozygous $Hb9^{nlslacZ}$ embryos, whereas in homozygous $Hb9^{nlslacZ}$ embryos, ~50% of LacZ cells coexpressed Chx10 (Figures 5B and 5C), and many of these cells also expressed Isl1 (Figures 5E and 5F). In homozygous $Hb9^{nlslacZ}$ embryos, MNs did not express En1, a marker of V1 neurons which derive from progenitors that do not express Lim3 (Ericson et al., 1997a; data not shown). Thus, the acquisition of interneuron properties by MNs appears specific to markers of V2 neuron identity. Since Lim3 and Gsh4 expression is eventually extinguished from somatic MNs in $Hb9^{nlslacZ}$ mutants, we examined whether the ectopic expression of Chx10 was also transient. Ectopic Chx10 expression was lost from MNs over the period E10.5–E13.5, whereas expression in V2 neurons persisted (Figures 5C and 5F; data not shown). Thus, in the absence of *Hb9* function, MNs maintain expression of Lim3 and Gsh4, albeit transiently, and apparently as a consequence, acquire expression of the V2 neuron marker Chx10.

The expression of Chx10 by MNs in *Hb9* mutants raised the issue of whether these neurons still project axons in an MN-like trajectory or acquire the projection pattern of V2 neurons, a class of ipsilateral spinal projection interneurons (K. Sharma et al., unpublished data). We therefore examined whether $Chx10^{+}/LacZ^{+}/Isl1^{+}$ neurons projected axons into the periphery in $Hb9^{nlslacZ}$ mutants. After injection of horseradish peroxidase (HRP) into the proximal region of the developing limb in E11.5 homozygous $Hb9^{nlslacZ}$ embryos, many $Chx10^{+}/Isl1/2^{+}$ neurons were labeled (Figures 5H and 5J). In contrast, in heterozygous $Hb9^{nlslacZ}$ mutants, labeled $Isl1/2^{+}/LacZ^{+}$ MNs did not express Chx10 (Figures 5G and 5I). These results show that in *Hb9* mutants, many neurons that express the V2 neuron marker Chx10 continue to project axons out of the ventral root and thus retain an axonal projection characteristic of MNs.

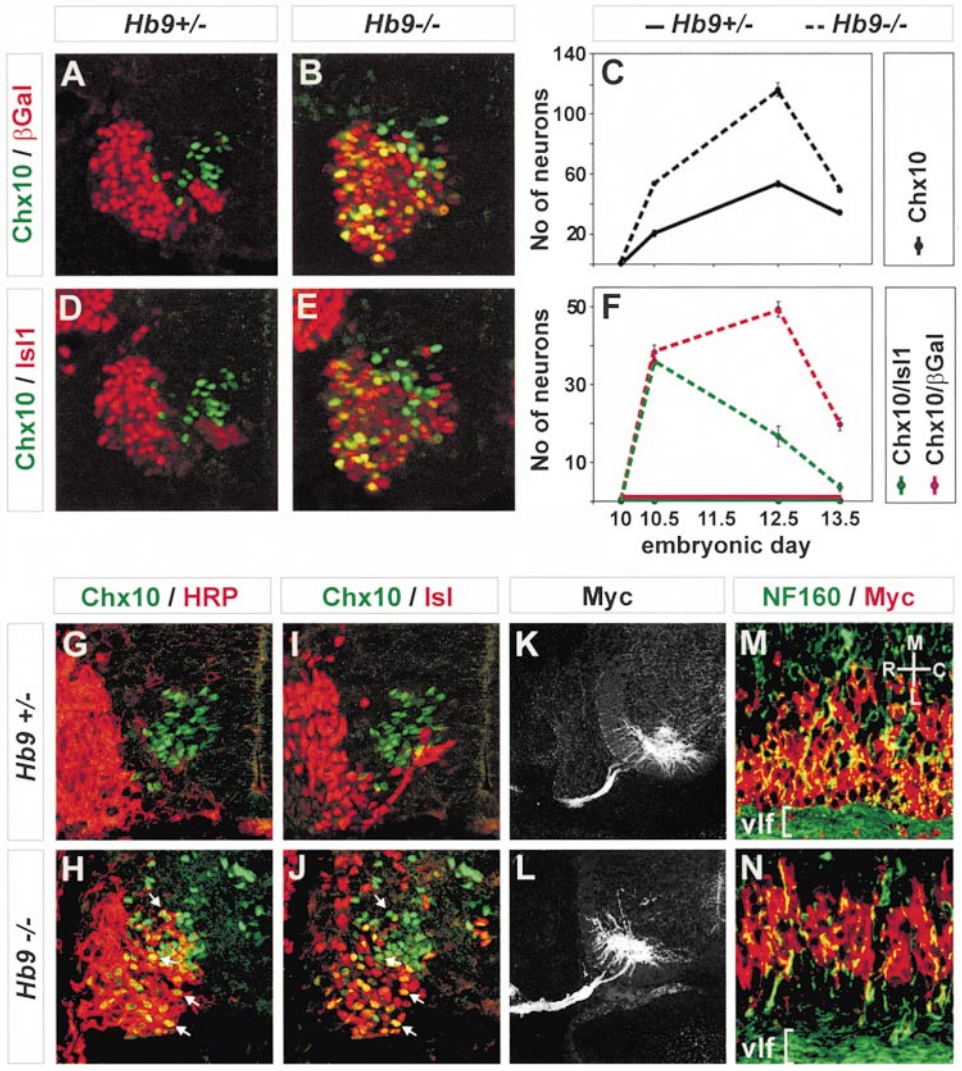

Figure 5. V2 Interneuron Marker Expression by MNs but No Accompanying Change in Axonal Trajectory in Mice Lacking *Hb9*

Analysis of Chx10 expression by β-gal-labeled cells and Isl1 MNs at different developmental stages in brachial spinal cord (level C7/8) of $Hb9^{nlslacZ/+}$ (A, C, D, and F) and $Hb9^{nlslacZ/nlslacZ}$ (B, C, E, and F) embryos.

(A, B, D, and E) Triple label immunocytochemical analysis of Chx10 (green), β-gal (red, [A and B]), and Isl1 (red, [D and E]) expression in sections of E10.5 spinal cord from $Hb9^{nlslacZ/+}$ (A and D) and $Hb9^{nlslacZ/nlslacZ}$ (B and E) embryos. In $Hb9^{nlslacZ/+}$ embryos, there is no coincidence of expression of β-gal or Isl1 with Chx10. In $Hb9^{nlslacZ/nlslacZ}$, many Isl1- and β-gal-labeled cells coexpress Chx10.

(C and F) Developmental time course of Chx10 expression in $Hb9^{nlslacZ/+}$ (solid lines) and $Hb9^{nlslacZ/nlslacZ}$ (dashed lines) embryos. The peak number of Chx10/β-gal cells in $Hb9^{nlslacZ/nlslacZ}$ embryos occurred at E10.5, after which their number gradually declined to that observed in $Hb9^{nlslacZ/+}$ embryos. Data from at least three independent sets of experiments are shown for each developmental stage (E10, E10.5, E12.5, and E13.5). For each stage, the number of labeled cells per ventral quadrant of the spinal cord was counted on at least four consecutive sections.

(G–N) Retrograde HRP labeling from the base of the forelimb of E11.5 heterozygous $Hb9^{nlslacZ}$ (G and I) and homozygous $Hb9^{nlslacZ}$ (H and J) embryos. Triple label immunocytochemical detection of Chx10 (green), HRP (red, [G and H]), and Isl1 (red, [I and J]) on the same section (G and I, and H and J). Arrows point to Chx10/HRP colabeled cells, two of which do not express Isl1.

(K–N) Axonal projection of *Hb9* neurons in $Hb9^{taumyc/+}$ (K and M) and $Hb9^{taumyc/taumyc}$ (L and N) embryos, detected using anti-Myc epitope antibodies. (K and L) Transverse sections of E13.5 spinal cord show Myc-labeled axons projecting into the ventral roots.

(M and N) Parasagittal sections of E13.5 spinal cord showing MN cell bodies and intersegmental projections in the vlf (white bar). Myc-labeled (red) axons are not detected among the neurofilament 160–labeled (green) axons in the vlf in $Hb9^{taumyc/taumyc}$ embryos, indicating the absence of intersegmental projections of ectopic Chox10 neurons. HRP injection into the vlf of the spinal cord of E13.5 wild-type embryos labels ipsilateral Chx10 neurons at more caudal segmental levels (data not shown). Abbreviations: R, rostral; C, caudal; M, medial; and L, lateral.

These findings do not exclude, however, that a fraction of the Chx10 MNs in homozygous $Hb9^{nlslacZ}$ embryos acquired an axonal trajectory characteristic of V2 neurons. To test this, we analyzed parasagittal sections through the ventrolateral funiculus (vlf) of the spinal cord of E12.5 heterozygous and homozygous $Hb9^{taumyc}$ embryos. We used the $Hb9^{taumyc}$ allele for this analysis since the intensity of labeling and discrimination of intraspinal axons were greater than with the $Hb9^{taulacZ}$ allele (data not shown). In both heterozygous and homozygous $Hb9^{taumyc}$

embryos, Myc-labeled axons were detected in the ventral roots (Figures 5K and 5L), but Myc-labeled intersegmental axons in the ventral funiculus were not detected (Figures 5M and 5N; data not shown). Thus, the ectopic expression of Chx10 by MNs appears not to be sufficient to reroute axons along an intraspinal trajectory.

The Emergence of MN Subtype Identity Is Disrupted in *Hb9* Mutants

The early alteration in migratory behavior and in the profile of transcription factor expression by MNs in *Hb9* mutants prompted us to examine whether the later molecular programs that define aspects of MN identity are affected. We first examined whether the profile of expression of Isl1, a LIM-HD protein that is initially expressed by all postmitotic MNs, is altered at later stages in *Hb9* mutants.

Although the initial number of Isl1 MNs was not altered by the loss of HB9 function (Figure 4G), from E10.5 onward, there was a progressive decline in the number of Isl1 neurons. By E13.5, the number of Isl1 neurons detected in homozygous $Hb9^{nlslacZ}$ embryos was only ~30% of that in heterozygous or wild-type embryos (Figure 4G). The loss of Isl1 expression was not the consequence of the death of MNs since no increase in TdT-mediated dUTP nick end labeling– (TUNEL-) positive cells was detected in the ventral spinal cord over this period (data not shown), and the total number of LacZ cells was not reduced. Thus, despite the initial generation of MNs in normal numbers in homozygous $Hb9^{nlslacZ}$ embryos, a marked disruption in the dynamic profile of the expression of several LIM-HD proteins soon becomes evident.

By E12.5–E13.5, MNs have acquired distinct class, columnar, and pool identities that can be defined by the expression of specific molecular markers (Figure 6A). We therefore examined whether the expression of MN subtype markers is affected by the loss of HB9 function.

MN Class Identity

The segregation of spinal MNs into somatic and visceral classes was maintained in *Hb9* mutant embryos. Somatic MNs can be identified at E12.5 by the expression of Isl2 (Tsuchida et al., 1994), and at this stage, the number of Isl2 neurons was similar in homozygous and heterozygous $Hb9^{nlslacZ}$ mutants (Figures 6D and 6E; data not shown). Thus, somatic MN differentiation occurs in the absence of HB9 function.

In the spinal cord, visceral MNs are generated predominantly at thoracic levels and can be defined by their location within the intermediate region (Barber et al., 1991; Markham and Vaughn, 1991) and, molecularly, by their expression of β-nicotinamide adenine dinucleotide phosphate diaphorase (NADPH-d) activity (Wetts et al., 1995). The number of neurons in the intermediate spinal cord that expressed NADPH-d neurons was markedly reduced in $Hb9^{nlslacZ}$ mutants examined at E14–E17 (Figures 6F and 6G; data not shown). The loss of NADPH-d expression, however, was much more marked in medially located neurons, and many laterally located NADPH-d MNs were still detected (Figures 6F and 6G; data not shown). The extent of *ChAT* expression by MNs in medial regions of the intermediate spinal cord was also significantly reduced in $Hb9^{nlslacZ}$ mutants (Figures 6B and 6C; data not shown). LacZ neurons were, however, detected at approximately normal numbers within both the medial and lateral regions of the intermediate spinal cord in homozygous $Hb9^{nlslacZ}$ embryos (data not shown), suggesting that the differentiation rather than the generation of visceral MNs is affected by the loss of *Hb9* function. The generation and differentiation of visceral MNs at caudal hindbrain and cervical spinal cord levels were not affected in *Hb9* mutant embryos, consistent with the finding that cranial visceral MNs do not express HB9 (Briscoe et al., 1999).

MN Columnar Identity

We next examined the expression of molecular markers that define the columnar subtype identity of MNs. By E12.5–E13.5, Lim3 MNs are normally restricted to the medial MMC (Figure 6H), but in homozygous $Hb9^{nlslacZ}$ embryos, Lim3 MNs were more widely dispersed throughout the LMC domain (Figure 6I). Although this result could simply reflect the persistence of expression of Lim3 by many MNs, it provides evidence that neurons with a molecular profile characteristic of the medial MMC are displaced in *Hb9* mutants.

The differentiation of MNs within the LMC was also disturbed in *Hb9* mutants. At limb levels of the spinal cord, the expression of *Retinaldehyde dehydrogenase 2* (*RALDH2*), a generic marker of LMC neurons (Zhao et al., 1996; Sockanathan and Jessell, 1998), was markedly reduced in homozygous $Hb9^{nlslacZ}$ embryos (Figures 6J and 6K). Moreover, the differentiation of MNs within the lateral subdivision of the LMC, characterized by coexpression of Isl2 and Lim1, was also greatly reduced (Figures 6L and 6M). Nevertheless, some lateral LMC MNs were detected, suggesting that the columnar subdivision of the LMC is not completely abolished in *Hb9* mutants.

MN Pool Identity

Within the LMC, distinct motor pools can be distinguished by the expression of the ETS proteins PEA3 and ER81 (Lin et al., 1998; S. A. et al., unpublished data). Marked reductions in the expression of PEA3 and ER81 were detected in LMC MNs both at forelimb and hindlimb levels. At forelimb levels, for example, a medial LMC–derived motor pool that innervates the pectoralis muscle expresses PEA3 (Figure 6N). In homozygous $Hb9^{nlslacZ}$ embryos, PEA3 expression was almost completely absent from MNs at this axial level (Figure 6O). The disruption of ETS protein expression was generally more severe than the loss of columnar markers (data not shown). ER81 and PEA3 expression by subsets of DRG neurons was, however, not affected in homozygous $Hb9^{nlslacZ}$ embryos (Figures 6N and 6O; data not shown). Taken together, these results reveal that the elimination of HB9 function results, directly or indirectly, in a disruption in the establishment of the class, columnar, and pool identities of MNs.

Defects in Motor Axon Trajectories in *Hb9* Mutant Mice

What are the consequences of the marked disruption in the molecular program of MN differentiation for the connectivity of MNs? To begin to address this issue, we examined whether the projection of motor axons toward their peripheral targets is altered in *Hb9* mutant embryos.

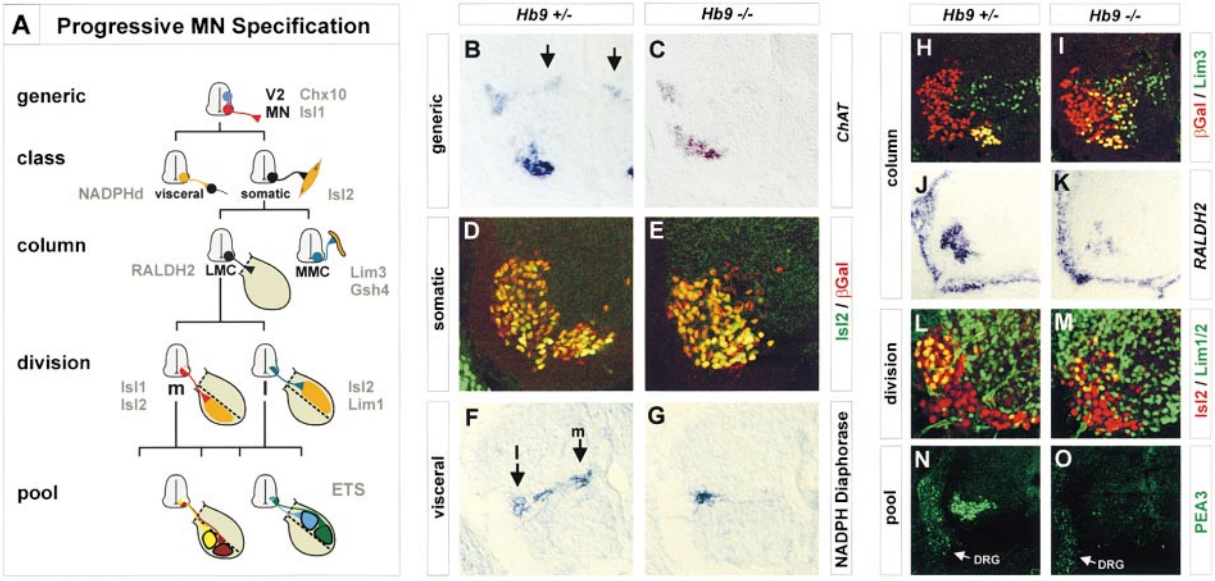

Figure 6. Defects in MN Subtype Identity in *Hb9* Mutant Mice

(A) Diagram summarizing sequential steps in MN differentiation in the developing spinal cord. MNs (red) initially acquire a generic identity that distinguishes them from neighboring interneurons (in this diagram, only V2 interneurons are shown). MNs initially express Isl1, whereas V2 neurons (blue) express Chx10. There are two major classes of spinal MNs, visceral and somatic, that project to different target cells. Most visceral MNs can be identified by expression of NADPH-d, and somatic MNs by expression of Isl2. The somatic MN class consists of two major columns, the MMC and the LMC, which project to skeletal muscles in different peripheral locations. LMC MNs can be identified by expression of *RALDH2*, and MMC neurons by expression of Lim3 and Gsh4. Within the LMC, neurons in the medial (m) division coexpress Isl1 and Isl2 and project to ventrally derived limb muscles, whereas neurons in the lateral (l) division coexpress Isl2 and Lim1 and project to dorsally derived limb muscles. Within each LMC division, MN pools that project to individual limb muscles can be identified by expression of the ETS domain proteins PEA3 and ER81. For details, see Tsuchida et al. (1994), Ericson et al. (1997a), Sockanathan and Jessell (1998), Lin et al. (1998), and the text.

(B–O) Expression of MN subtype markers in developing spinal MNs. Images show E13.5 thoracic spinal cord (B, C, F, and G), E12.5 C7/8 level spinal cord (D and E), and E13.5 C7/8 level spinal cord (H–O) in $Hb9^{nlslacZ/+}$ and $Hb9^{nlslacZ/nlslacZ}$ embryos.

(B and C) *ChAT* (generic MN marker) expression detected by in situ hybridization. Arrows in (B) point to medial populations of visceral MNs.

(D and E) β-gal cells (red) coexpress Isl2 (green; a somatic MN-specific marker at this stage). The number of Isl2 cells is similar in $Hb9^{nlslacZ/+}$ and $Hb9^{nlslacZ/nlslacZ}$ embryos examined at E12.5. By E13.5, the number of Isl2 cells in mutants is, however, reduced by ~40% compared with heterozygote embryos (data not shown).

(F and G) NADPH-d enzyme activity in visceral MNs. In heterozygous $Hb9^{nlslacZ}$ embryos, both lateral (l) and medial (m) populations of NADPH-d neurons are present (F). In homozygous $Hb9^{nlslacZ}$ embryos, NADPH-d expression is absent from medial regions of the intermediate zone (G) although many cells in this region still express LacZ (data not shown).

(H and I) Coexpression of Lim3 (green) and β-gal (red) delineates the medial MMC in heterozygous $Hb9^{nlslacZ}$ embryos (H). Lim3/β-gal cells in homozygous $Hb9^{nlslacZ}$ embryos are not restricted to the region of the medial MMC (I).

(J and K) In situ hybridization analysis of *RALDH2* expression delineates LMC neurons (J). There is a marked reduction of *RALDH2* expression in homozygous $Hb9^{nlslacZ}$ embryos (K).

(L and M) Coexpression of Isl2 (red) and Lim1/2 (green) delineates lateral LMC neurons (L). There is a marked reduction of Isl2/Lim1 cells in homozygous $Hb9^{nlslacZ}$ embryos (M).

(N and O) PEA3 expression (green; motor pool marker) by pectoralis MNs (N) is severely reduced in homozygous $Hb9^{nlslacZ}$ embryos (O). PEA3 expression by DRG neurons (arrows) is not affected in homozygous $Hb9^{nlslacZ}$ embryos.

In heterozygous $Hb9^{taulacZ}$ embryos examined at E11.5, the pattern of axonally transported *lacZ* expression coincided with the trajectories of somatic MNs (see Ericson et al., 1997a; Figure 7A; data not shown). For example, at hindbrain levels, the hypoglossal nerve, and at cervical spinal cord levels, the segmentally arrayed projections of somatic motor axons in the ventral roots, were delineated by LacZ expression (Figure 7A). LacZ-labeled peripheral motor axons were also detected in homozygous $Hb9^{taulacZ}$ embryos (Figures 7B–7D; data not shown), indicating that HB9 is not required for the initial projection of motor axons into the periphery. However, there were marked, albeit variable, defects in the more distal projections of motor axons in homozygous $Hb9^{taulacZ}$ embryos (Figures 7B–7D; data not shown). One of the most dramatic instances of the variability of the defects in motor axon trajectory was detected at caudal hindbrain levels. The hypoglossal motor nerve was either completely absent or severely misrouted in some *Hb9* mutant embryos (Figure 7B; data not shown), but present, with an apparently normal trajectory, in others (Figure 7C).

The disruption in motor axon trajectories in *Hb9* mutants led us to examine whether the major branches of somatic motor axons to axial and limb regions were formed. Analysis of the pattern of motor nerve branching in embryos stained in both whole-mount and transverse sections revealed a marked defect in the organization of motor nerves at the axial muscle branchpoint and at

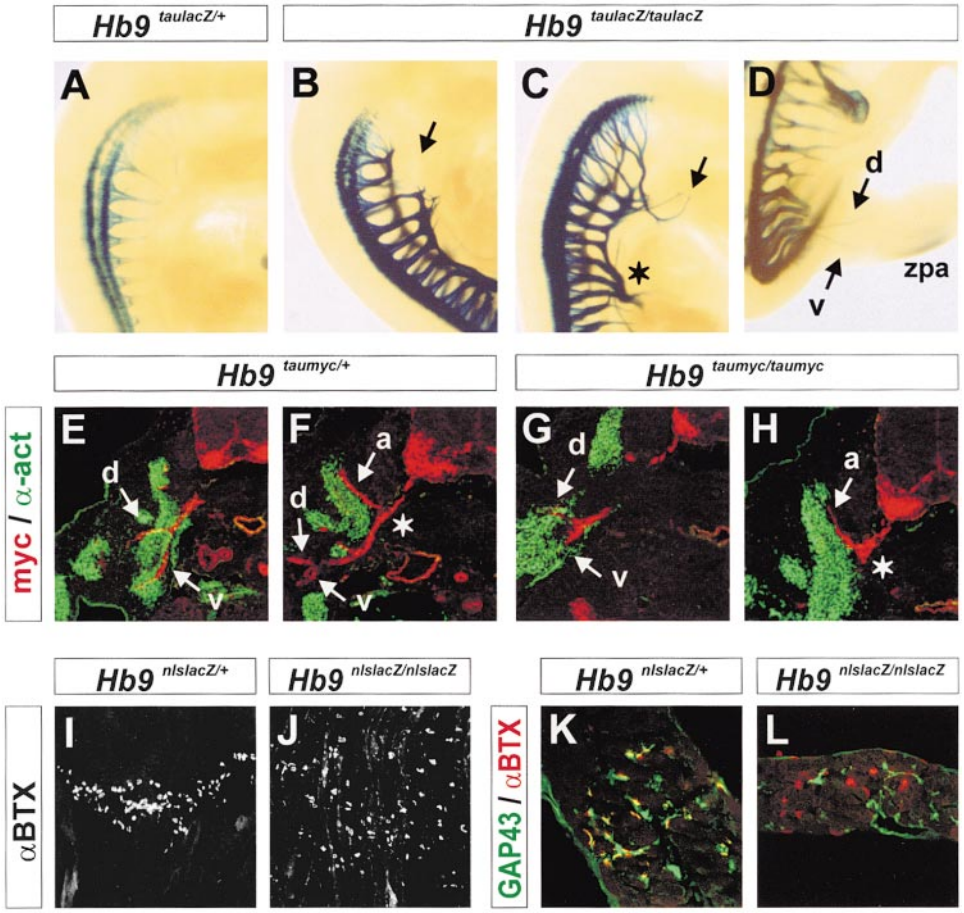

Figure 7. Defects in Motor Axon Projections in *Hb9* Mutant Mice

(A–D) Whole-mount β-gal staining of $Hb9^{taulacZ}$ embryos.

(A–C) Perturbation in motor axon projections in E11.5 $Hb9^{taulacZ/taulacZ}$ embryos (B and C), when compared with the axonal projection pattern observed in $Hb9^{taulacZ/+}$ embryos (A). Arrows point to the hypoglossal nerve, which is absent or misrouted in some mutants (B) but present in others (C). Asterisk in (C) indicates expanded plexus region at the base of the forelimb.

(D) Dorsal (d) and ventral (v) motor axon branches in the hindlimb of an E12.5 $Hb9^{taulacZ/taulacZ}$ embryo. Note β-gal labeling in the zone of polarizing activity (zpa) of the developing limb.

(E–H) Analysis of peripheral projections of motor axons in sections of E12.5 $Hb9^{taumyc/+}$ (E and F) and $Hb9^{taumyc/taumyc}$ (G and H) embryos. Double label immunocytochemical detection of Myc-labeled (red) axons projecting toward skeletal muscles (α-actinin-labeled; green). Axial muscle nerve branches are indicated (arrows, [a]). Star indicates the expansion of the axial nerve branch point (H). The dorsally (d) and ventrally (v) directed branches of motor axons in the limb are evident in *Hb9* heterozygous (E) and homozygous (G) mutant embryos.

(I–L) Analysis of innervation of diaphragm muscle of postnatal day 0 heterozygous (I and K) and homozygous $Hb9^{nlslacZ}$ (J and L) mice.

(I and J) Whole-mount α-BTX staining shows the presence of AChR clusters localized in a tight band in the diaphragm of heterozygous embryos (I) and a scattered distribution of AChR clusters over a larger region of the diaphragm muscle in homozygous $Hb9^{nlslacZ}$ embryos (J).

(K and L) Double label immunocytochemical detection of GAP-43-labeled axons and nerve terminals (green) and α-BTX-labeled AChR clusters (red). Transverse section through the diaphragm reveals the coincidence (yellow patches) of GAP-43 and α-BTX labeling in heterozygous muscle (K) and the lack of coincidence of label in homozygous $Hb9^{nlslacZ}$ embryos (L).

the plexus region at the base of the fore- and hindlimbs. In heterozygous $Hb9^{taulacZ}$ and $Hb9^{taumyc}$ embryos, motor axons at these plexus regions formed a tight fascicle (Figures 7A, 7E, and 7F), whereas in homozygous embryos, motor axons were dispersed and defasciculated (Figures 7B, 7C, 7G, and 7H; data not shown). Nevertheless, motor axon projections to axial muscles were detectable in homozygous $Hb9^{taulacZ}$ and $Hb9^{taumyc}$ embryos (Figures 7E–7H; data not shown). Similarly, distinct motor axon branches projected into the dorsal and ventral halves of the limb mesenchyme in *Hb9* mutant embryos (Figures 7D and 7G). Thus, there are marked defects in the peripheral organization of motor nerves at sites of critical motor axon pathfinding decisions, although the major peripheral axon branches of somatic MNs are present.

Defects in Muscle Innervation by Motor Axons in *Hb9* Mutants

The defect in the peripheral organization of motor nerve branches in *Hb9* mutants led us to examine whether there are also defects in the innervation of target muscles. We first analysed the innervation of limb muscles in late embryonic stage (E17.5) embryos, using GAP-43

expression to visualize peripheral axons and α-bungarotoxin (α-BTX) labeling to delineate clusters of acetylcholine receptors (AChR) on the muscle surface. We detected no obvious defect in the pattern of motor innervation or in AChR expression in fore- and hindlimb muscles in *Hb9* mutant embryos (data not shown).

Hb9 mutant mice die soon after birth with uninflated lungs, and we therefore considered the possibility that the innervation of the diaphragm muscle by phrenic MNs might be affected. In the diaphragms of wild-type and heterozygous $Hb9^{nlslacZ}$ neonates, AChR clusters were restricted to a central domain of the muscle that coincided with the position of muscle innervation (Figure 7I). In contrast, in homozygous $Hb9^{nlslacZ}$ mice, AChR clusters were present but distributed over a much wider region of the muscle surface (Figure 7J). Many of these scattered AChR clusters were abnormally small (Figure 7J; data not shown), and the thickness of the diaphragm muscle was markedly reduced in homozygous $Hb9^{nlslacZ}$ embryos (Figures 7K and 7L). In addition, in the diaphragms of wild-type and heterozygous $Hb9^{nlslacZ}$ mice, AChR clusters were invariably associated with GAP-43-labeled nerve terminals (Figure 7K). In contrast, in homozygous $Hb9^{nlslacZ}$ mice, many AChR clusters were not associated with GAP-43-labeled nerve branches (Figure 7L). Extensive axonal sprouting was also detected in regions of the diaphragm close to the point of entry of the phrenic nerve (data not shown). These observations reveal a marked defect in the innervation of certain skeletal muscles in *Hb9* mutant embryos. They also raise the possibility that the perinatal lethality of *Hb9* mutant animals results, at least in part, from the diaphragm denervation phenotype.

Discussion

This paper provides evidence that many aspects of the differentiation of postmitotic MNs in the mammalian spinal cord depend on functions provided by the homeobox gene *Hb9*. Our findings add to an understanding of the molecular steps of MN differentiation in two main ways. They provide genetic evidence that the signals involved in the generation of MNs can be dissociated from the later steps that consolidate MN identity. In addition, they provide evidence that a transcription factor expressed at an early stage in the differentiation of all spinal MNs has an essential function in the acquisition of MN subtype identities. Thus, they provide an initial insight into the hierarchical relationship of the transcription factors that define distinct functional subsets of MNs in the developing spinal cord. We discuss the possible roles of HB9 in the progressive specification of MN identity that are suggested by this analysis of the *Hb9* mutant phenotype.

A Requirement for HB9 Function in Early MN Development

At the earliest stages of MN genesis, late-stage $Lim3^{+}$ MN progenitors express HB9. However, during the peak period of MN generation, the onset of HB9 expression by most cells appears to occur after that of Lim3 and coincident with that of Isl1, apparently in newly generated postmitotic MNs. Consistent with this, the loss of *Hb9* function has no discernible effect on the number of spinal MNs initially generated. Thus, the phenotype of *Hb9* mutant mice supports the idea that the relevant period of expression and function of HB9 is in postmitotic MNs. Previous studies have analyzed MN differentiation in mice lacking Isl1, a LIM-HD protein expressed almost exclusively by postmitotic MNs. However, in *Isl1* mutant mice, MNs undergo rapid apoptotic death (Pfaff et al., 1996; J. Ericson et al., unpublished data), hindering an analysis of later steps in MN differentiation. Isl1 is initially expressed by MNs in *Hb9* mutant mice, but many neurons rapidly lose Isl1 expression. Despite this, MNs survive. This result, taken together with the more drastic MN phenotype of *Isl1* mutant mice, suggests that MNs may require Isl1 for their survival only during a brief critical period, soon after cell cycle exit.

A Role for HB9 in the Consolidation of the MN–V2 Interneuron Identity Decision

The progenitors of both MNs and V2 interneurons are marked by expression of Lim3 (and the functionally redundant protein Gsh4), implying that additional factors are required to select between these two neuronal fates. The analysis of changes in transcription factor expression by postmitotic MNs in *Hb9* mutant embryos provides support for the idea that emerged from studies in chick (Tanabe et al., 1998) that the MNR2/HB9 class of homeodomain proteins has a role in selecting MN rather than V2 interneuron identity within the ventral spinal cord. In the chick, ectopic expression of MNR2 and HB9 suppresses the generation of V2 interneurons and promotes MN differentiation, providing gain-of-function evidence that MNR2 and HB9 have such a neuronal subtype selector function. The present studies provide complementary loss-of-function evidence that HB9 serves such a function in MNs, acting to repress the expression of V2 interneuron character and thus to consolidate MN fate (Figure 8). These results have the additional implication that the stabilization of MN rather than V2 interneuron identity may not be achieved until after MNs have left the cell cycle.

At a molecular level, the HB9-dependent consolidation of MN phenotype is likely to be mediated through the regulation of Lim3 (and Gsh4) (Figure 8). In *Hb9* mutant embryos, the expression of Lim3 and Gsh4 persists in postmitotic MNs for an abnormally long period, implying that HB9 normally functions, directly or indirectly, to repress the expression of Lim3 and Gsh4. In the chick, ectopic expression of Lim3 is sufficient to induce V2 interneuron markers in a cellular context in which MNR2 and other MN homeodomain proteins are not expressed (Tanabe et al., 1998). It is likely, therefore, that the persistence of Lim3 and Gsh4 expression in *Hb9* mutants is responsible for the ectopic expression of Chx10 by MNs (Figure 8). Nevertheless, MNs do not undergo a complete switch to a V2 interneuron identity in *Hb9* mutants. The incomplete and transient nature of the switch to a V2 interneuron identity may reflect the prior action of progenitor cell factors that initiate the process of MN specification.

An important issue raised by our findings is that of the respective roles of HB9 in the development of mouse and chick MNs. In the chick, HB9 expression is restricted

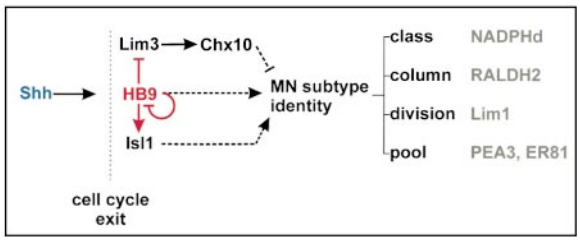

Figure 8. Functions of HB9 in the Differentiation of Postmitotic MNs

Proposed functions of HB9 in postmitotic MNs. Red arrows highlight the steps in MN differentiation that appear to be controlled by HB9. HB9 appears to have two main, possibly interrelated, functions. First, HB9 is normally required for the rapid downregulation of Lim3 (and Gsh4) from most postmitotic MNs, which in turn appears to prevent expression of the V2 interneuron marker Chx10. One exception to this function of HB9 is in the context of medial MMC neurons, in which Lim3 and Gsh4 expression persists in MNs for a prolonged period, even in wild-type embryos (Tsuchida et al., 1994; Sharma et al., 1998). Thus, medial MMC neurons appear to be subject to distinct regulatory controls on the timing of Lim3/Gsh4 expression and, by inference, on the suppression of V2 interneuron character. Second, HB9 is required for the maintenance of Isl1 expression in postmitotic MNs. A negative autoregulatory activity of HB9 is also shown and is indicated as a direct interaction although it may be mediated indirectly. Approximate timing of cell cycle exit with respect to homeodomain protein expression is indicated. HB9 is also required, directly or indirectly, for the efficient establishment of the class, columnar, divisional, and pool identities of spinal MNs. Dashed lines indicate that the erosion of MN subtype identity could reflect a direct action of HB9, the loss of expression of proteins, such as Isl1, that normally serve a positive function in MN differentiation or the ectopic expression of interneuron markers such as Chx10, or a combination of these events. Proteins indicated in gray delineate markers of MN subtype identity that are affected in *Hb9* mutants. Abbreviation: Shh, Sonic hedgehog, an inductive signal required for MN generation and HB9 expression. For further details, see text.

to postmitotic MNs, whereas MNR2 expression is detected at a much earlier stage, in MN progenitors (Tanabe et al., 1998). In contrast, in mouse, HB9 expression is detected in some MN progenitors at early stages of MN genesis. However, for the peak period of MN generation, our data provide evidence that the expression of HB9 is delayed with respect to that of Lim3 and appears coincident with that of Isl1. Thus, HB9 appears to be expressed at a slightly earlier stage in the progression of MN differentiation in mouse than its counterpart in chick. Nevertheless, the profile of expression of mouse HB9 does not include an early and prominent phase of expression in MN progenitors, a profile characteristic of chick MNR2. A mouse MNR2 homolog has not been isolated to date, however (C. William and Y. Tanabe, personal communication). Thus, we cannot exclude that in mouse, HB9 has subsumed the functions performed in chick by MNR2. If this is the case, the finding that MNs are generated in normal numbers in *Hb9* mutants would argue for the existence of an MNR2/HB9-independent pathway of MN generation. As discussed previously (Tanabe et al., 1998), such a pathway must operate at least in the hindbrain since neither mouse nor chick cranial visceral MNs, nor their progenitors, express MNR2 or HB9 (Tanabe et al., 1998; Briscoe et al., 1999). The ability of MNR2 and HB9 to induce a coordinate program of MN differentiation in chick spinal cord, together with the MN phenotype detected in *Hb9* mutant mice, does, however, support the idea that this homeodomain protein subfamily has an important if as yet incompletely defined role in early MN differentiation.

The Acquisition of MN Subtype Identities Is Impaired in *Hb9* Mutant Mice

The early postmitotic period of MN development is accompanied by the differentiation of functional subsets of MNs that can be defined both by their anatomical organization and by expression of specific molecular markers (see Figure 6A). Many aspects of the differentiation of distinct MN subtypes, including columnar divisional and pool identities, are markedly affected by the loss of *Hb9* function (Figure 8).

These defects in MN subtype identity could simply be an indirect consequence of the persistence of expression of Lim3 and Gsh4 and/or the ectopic expression of Chx10. Nevertheless, defects in the columnar and pool identities of MNs are evident well after the phase of deregulation of Lim3, Gsh4, and Chx10 has subsided. Thus, it remains possible that HB9 has a more direct role in the specification of MN subtype identity. HB9 could, for example, function as a cofactor in a series of independent molecular programs that regulate the emergence of columnar, divisional, and pool subtype identities. Alternatively, HB9 could act at an early point in an obligate sequential program of somatic MN differentiation that progresses from columnar to divisional to pool identity. One line of evidence that argues against a strict requirement for sequential programs of MN subtype differentiation derives from the observation that retinoids appear able to impose a lateral LMC character on thoracic level MNs that have not acquired a generic LMC character (Sockanathan and Jessell, 1998). Thus, MN divisional character, at least, may be acquired independently of columnar character.

The proposed roles of the MNR2/HB9 proteins in regulating MN subtype identity may have some parallels with the functions of the Phox2a/b homeodomain proteins in the specification of sympathetic neuronal fate (Goridis and Brunet, 1999; Lo et al., 1999; Pattyn et al., 1999). Phox2 proteins are necessary for the induction of transmitter-synthetic enzymes and other features of sympathetic neuronal differentiation. In addition, at hindbrain levels, the Phox2 proteins are expressed selectively by visceral MNs in a pattern complementary to that of MNR2 and HB9 (Briscoe et al., 1999; Goridis and Brunet, 1999). It is possible, therefore, that the segregated expression of these two families of homeodomain proteins contributes to distinctions in the somatic and visceral subtype identity of cranial MNs.

Perturbed MN Migration and Axonal Projections in *Hb9* Mutants

The loss of *Hb9* function results in marked defects in the migratory and settling patterns of spinal MNs. The most striking migratory defect in *Hb9* mutants is the failure of many MN cell bodies to be retained within the spinal cord. These defects in MN migration are accompanied by marked errors in the pattern of axonal projections of somatic MNs. There is, however, variability in the precise nature of the errors in motor axon projection

between mutant embryos. One consistent axonal projection phenotype in the spinal cord of *Hb9* mutant mice is a pronounced defasciculation of axons, evident at the branchpoint of axial and limb-directed motor axons and also at the plexus region at the base of the limbs. This finding raises the possibility that adhesive interactions between motor axons and/or the ability of motor axons to respond to extrinsic guidance cues are impaired in *Hb9* mutants.

Despite these defects, each of the major axonal branches of spinal somatic MNs, to axial muscles and to dorsal and ventral limb muscles, is present in *Hb9* mutant embryos. The detection of overtly normal projections to axial muscles is not surprising since these axons originate from medial MMC neurons, which normally retain expression of Lim3 and Gsh4 (Tsuchida et al., 1994; Ericson et al., 1997b; Sharma et al., 1998). The detection in *Hb9* mutant embryos of both dorsally and ventrally directed motor axon branches in the limb may reflect, in part, the residual differentiation of some lateral LMC neurons. Nevertheless, the axons of many MNs that have lost their LMC identities also appear able to make either dorsal or ventral projections into the limb bud. This finding is consistent with previous studies showing that thoracic level MNs that are committed to a MMC identity form dorsal and ventral axonal projections in the limb when transplanted to limb levels (O'Brien and Oppenheim, 1990; O'Brien et al., 1990; Ensini et al., 1998). It seems possible, therefore, that the acquisition of LMC divisional identity provides MNs with the ability to select appropriately a dorsal or ventral trajectory, rather than embarking along one or another trajectory at random. The necessity for motor axons to project along either a dorsal or ventral path in the limb may reflect the presence of a nonpermissive environment for axons in the central core of the developing limb mesenchyme (see Tosney and Landmesser, 1985).

Taken together, our studies provide evidence that HB9 has an essential role in consolidating the identity of spinal MNs and, in particular, in suppressing the expression of V2 interneuron character. Since HB9 expression persists in adult MNs, it is possible that its activities help to maintain the differentiated properties of MNs into postnatal and adult life. Defining the direct downstream targets of HB9 may help to clarify further how the molecular and functional properties of MN subtypes are established.

Experimental Procedures

Generation of *Hb9* Mutant and Transgenic Mice

Mouse genomic clones used in the generation of *Hb9* mutant mice and transgenic lines were derived from a 129/Sv genomic library (Stratagene). The transgenic TgN(Hb9)SAX16 line was derived from a construct that used a 9 kb NotI fragment comprising the 5′ upstream region of the *Hb9* gene inserted 5′ to an IRES-*nlslacZ* cassette (see below). The targeting vector for the production of *Hb9* mutant mice was constructed from genomic fragments derived from a 9 kB NotI fragment 5′ to the first exon of *Hb9* and a HindIII clone overlapping with the 5′ clone but extending into the 3′ region of *Hb9*. A 6 kB 5′ Sse83871-NotI fragment spanning into the first exon of *Hb9* and an adjacent 3 kB 3′ NotI–XbaI fragment were cloned into a vector containing a PmeI site for linearization of the targeting constructs. NotI- or PacI-flanked targeting cassettes were generated independently (and comprised IRES-*nlslacZ*, IRES-*taulacZ*, IRES-*taumyc*, an SV40 polyadenylation signal, and a lox-flanked *pgk-neo* cassette). These cassettes were integrated into the basic targeting construct.

For the generation of expression cassettes, marker genes were inserted downstream of an IRES from encephalomyocarditis virus (Ghattas et al., 1991), in frame with the ATG of a NcoI site at the 3′ end of the IRES (Mombaerts et al., 1996). Linearized targeting constructs were electroporated into W9.5 ES, cells selected with G418, and screened for potential recombinants by Southern blot analysis. A 1 kB 3′ XbaI–XhoI fragment was used as a probe to screen for ES cell recombinants (SalI/XhoI digest). This probe generates a 20 kB wild-type band and a 6 kB mutant band. The average frequency of recombination for the four constructs described in this study was ~1:20. Recombinant clones were injected into C57BL/6J blastocysts to generate chimeric founders that transmitted the mutant allele. All experiments presented in this study involved analysis of embryos derived from heterozygous 129Sv × C57BL/6J intercrosses.

A 5′ Fragment of the *Hb9* Gene Confers MN–Specific Transgene Expression

A ~9 kb Not1 fragment of *Hb9* (Figures 2A and 2Bi) was sufficient to direct an SV40–*nlslacZ* fusion protein to developing MNs in transgenic mouse embryos examined at E10 (Figure 2C; data not shown). The pattern of *lacZ* corresponded closely to the expression of endogenous HB9 (Figures 1 and 2C; data not shown). The restriction of transgene expression to somatic MNs was apparent at this stage at caudal hindbrain levels at which LacZ, like HB9, was expressed by somatic hypoglossal MNs but was excluded from visceral vagal MNs (Briscoe et al., 1999; data not shown). At sacral levels of E9.5–E10.5 embryos, both endogenous HB9 expression and LacZ expression in transgenic mice were detected throughout the neural tube, in the notochord and also in the primitive gut tube (data not shown).

In Situ Hybridization, Histochemistry, and Immunocytochemistry

For in situ hybridization analysis, sections were hybridized with mouse *RALDH2*- and *ChAT*-specific digoxigenin-labeled probes (Schaeren-Wiemers and Gerfin-Moser, 1993). Antibodies used in this study were monoclonal immunoglobulin G anti-HB9 (N-terminal); rabbit anti-HB9 (C-terminal; kindly provided by S. Pfaff); Pax6; MPM2; NF160; BrdU-FITC (Ericson et al., 1997a; Tanabe et al., 1998); skeletal α-actinin (Sigma); anti-Lim1/2 (Tsuchida et al., 1994); rabbit anti-Lim3; Isl1/2; Isl2; HB9 (N-terminal); Nkx2.2; Chx10; Brn3.0 (Ericson et al., 1997a; Tanabe et al., 1998); GAP-43 (Aigner et al., 1995); PEA3 (S. A. et al., unpublished data) generated against the 14 C-terminal amino acids of mouse PEA3 coupled to keyhole limpet hemocyanin (KLH), used at 1:1000; Myc (S. Morton and T. M. J., unpublished data) generated against the Myc epitope (Evan et al., 1985) coupled to KLH, used at 1:8000; β-gal (Cappel); goat anti-β-gal (Arnel); HRP (Jackson Labs); and guinea pig anti-Isl1 (Tanabe et al., 1998). Cryostat sections were processed for immunohistochemistry as described (Tsuchida et al., 1994) using fluorophore-conjugated secondary antibodies (Jackson Labs) (1:500 to 1:1000). Rhodamine-labeled α-BTX (Jackson Labs) was used at 1:2000. Images were collected on a BioRad MRC 1024 confocal microscope.

BrdU Labeling and Histology

BrdU experiments were performed by intraperitoneal injection of BrdU (Sigma; 50 μg/g body weight) 2 hr before sacrifice. Detection of BrdU was performed as previously described (Sockanathan and Jessell, 1998). TUNEL assays were performed with a kit from Boehringer, NADPH-d reactions were performed as described (Wetts et al., 1995), and β-gal whole-mount staining was performed as described (Mombaerts et al., 1996).

Retrograde Neuronal Labeling

HRP (20%; Boehringer)/Isolecithin (1%) in phosphate-buffered saline was injected into the limbs of E11.5 mouse embryos or into the ventral funiculus of E13.5 spinal cord and incubated for 2–4 hr as described (Landmesser, 1978b) before fixation and immunocytochemical detection of HRP.

Acknowledgments

We thank S. Morton and C. William for antibodies, S. Kaplan for expert technical assistance, C. Stewart for W9.5 cells, and J. Kehrl for communication of unpublished results. We are grateful to S. Pfaff for ongoing discussions, for providing an anti-C-terminal HB9 antiserum, and for initial studies that contributed to the characterization of the 9 kb regulatory region of *Hb9*. K. MacArthur and I. Schieren provided expert help in preparing the manuscript and figures, and J. Briscoe, P. Caroni, and K. Lee provided helpful comments on the manuscript. S. S. and T. M. J. are supported by grants from the National Institutes of Health, and S. A. is supported by a grant from the Swiss National Science Foundation and a Human Frontiers Scientific Program Fellowship. T. M. J. is an Investigator of the Howard Hughes Medical Institute.

Received April 29, 1999; revised June 24, 1999.

References

Aigner, L., Arber, S., Kapfhammer, J.P., Laux, T., Schneider, C., Botteri, F., Brenner, H.R., and Caroni, P. (1995). Overexpression of the neural growth–associated protein GAP-43 induces nerve sprouting in the adult nervous system of transgenic mice. Cell *83*, 269–278.

Appel, B. (1999). LIMitless combinations? Neuron *22*, 3–5.

Barber, R.P., Phelps, P.E. and Vaughn, J.E. (1991). Generation patterns of immunocytochemically identified cholinergic neurons at autonomic levels of the rat spinal cord. J. Comp. Neurol. *311*, 509–519.

Briscoe, J., Sussel, L., Serup, P., Hartigan-O'Connor, D., Jessell, T.M., Rubenstein, J.L., and Ericson, J. (1999). Homeobox gene Nkx2.2 and specification of neuronal identity by graded Sonic hedgehog signalling. Nature *398*, 622–627.

Cepko, C.L. (1999). The roles of intrinsic and extrinsic cues and bHLH genes in the determination of retinal cell fates. Curr. Opin. Neurobiol. *9*, 37–46.

Edlund, T., and Jessell, T.M. (1999). Progression from extrinsic to intrinsic signaling in cell fate specification: a view from the nervous system. Cell *96*, 211–224.

Ensini, M., Tsuchida, T.N., Belting, H.G., and Jessell, T.M. (1998). The control of rostrocaudal pattern in the developing spinal cord: specification of motor neuron subtype identity is initiated by signals from paraxial mesoderm. Development *125*, 969–982.

Ericson, J., Thor, S., Edlund, T., Jessell, T.M., and Yamada, T. (1992). Early stages of motor neuron differentiation revealed by expression of homeobox gene Isl1. Science *256*, 1555–1560.

Ericson, J., Morton, S., Kawakami, A., Roelink, H., and Jessell, T.M. (1996). Two critical periods of sonic hedgehog signaling required for the specification of motor neuron identity. Cell *87*, 661–673.

Ericson, J., Rashbass, P., Schedl, A., Brenner-Morton, S., Kawakami, A., van Heyningen, V., Jessell, T.M., and Briscoe, J. (1997a). Pax6 controls progenitor cell identity and neuronal fate in response to graded Shh signaling. Cell *90*, 169–180.

Ericson, J., Briscoe, J., Rashbass, P., van Heyningen, V., and Jessell, T.M. (1997b). Graded sonic hedgehog signaling and the specification of cell fate in the ventral neural tube. Cold Spring Harbor Symp. Quant. Biol. *62*, 451–466.

Evan, G.I., Lewis, G.K., Ramsay, G., and Bishop, J.M. (1985). Isolation of monoclonal antibodies specific for human c-myc proto-oncogene product. Mol. Cell. Biol. *5*, 3610–3616.

Ghattas, I.R., Sanes J.R., and Majors, J.E. (1991). The encephalomyocarditis virus internal ribosome entry site allows efficient coexpression of two genes from a recombinant provirus in cultured cells and in embryos. Mol. Cell. Biol. *11*, 5848–5859.

Goridis, C., and Brunet, J.F. (1999). Transcriptional control of neurotransmitter phenotype. Curr. Opin. Neurobiol. *9*, 47–53.

Goulding, M. (1998). Specifying motor neurons and their connections. Neuron *21*, 943–946.

Harrison, K.A., Druey, K.M., Deguchi, Y., Tuscano, J.M., and Kehrl, J.H. (1994). A novel human homeobox gene distantly related to proboscipedia is expressed in lymphoid and pancreatic tissues. J. Biol. Chem. *269*, 19968–19975.

Landmesser, L. (1978a). The distribution of motorneurons supplying chick hind limb muscles. J. Physiol. *284*, 371–389.

Landmesser, L. (1978b). The development of motor projection patterns in the chick hind limb. J. Physiol. *284*, 391–414.

Lin, J.H., Saito, T., Anderson, D.J., Lance-Jones, C., Jessell, T.M., and Arber, S. (1998). Functionally related motor neuron pool and muscle sensory afferent subtypes defined by coordinate ETS gene expression. Cell *95*, 393–407.

Liu, I.S., Chen, J.D., Ploder, L., Vidgen, D., van der Kooy, D., Kalnins, V.I., and McInnes, R.R. (1994). Developmental expression of a novel murine homeobox gene (Chx10): evidence for roles in determination of the neuroretina and inner nuclear layer. Neuron *13*, 377–393.

Lo, L., Tiveron, M.C., and Anderson, D.J. (1998). MASH1 activates expression of the paired homeodomain transcription factor Phox2a, and couples pan-neuronal and subtype-specific components of autonomic neuronal identity. Development *125*, 609–620.

Lo, L., Morin, X., Brunet, J.-F., and Anderson, D.J. (1999). Specification of neurotransmitter identity by Phox2 proteins in neural crest stem cells. Neuron *22*, 693–705.

Markham, J.A., and Vaughn, J.E. (1991). Migration patterns of sympathetic preganglionic neurons in embryonic rat spinal cord. J. Neurobiol. *22*, 811–822.

Mombaerts, P., Wang, F., Dulac, C., Chao, S.K., Nemes, A., Mendelsohn, M., Edmondson, J., and Axel, R. (1996). Visualizing an olfactory sensory map. Cell *87*, 657–686.

Nornes, H.O., and Carry, M. (1978). Neurogenesis in spinal cord of mouse: an autoradiographic analysis. Brain Res. *159*, 1–6.

O'Brien, M.K., and Oppenheim, R.W. (1990). Development and survival of thoracic motoneurons and hindlimb musculature following transplantation of the thoracic neural tube to the lumbar region in the chick embryo: anatomical aspects. J. Neurobiol. *21*, 313–340.

O'Brien, M.K., Landmesser, L., and Oppenheim, R.W. (1990). Development and survival of thoracic motoneurons and hindlimb musculature following transplantation of the thoracic neural tube to the lumbar region in the chick embryo: functional aspects. J. Neurobiol. *21*, 341–355.

Pattyn, A., Morin, X., Cremer, H., Goridis, C., and Brunet, J.F. (1999). The homeobox gene Phox2b is essential for the development of autonomic neural crest derivatives. Nature *399*, 366–370.

Pfaff, S.L., Mendelsohn, M., Stewart, C.L., Edlund, T., and Jessell, T.M. (1996). Requirement for LIM homeobox gene Isl1 in motor neuron generation reveals a motor neuron–dependent step in interneuron differentiation. Cell *84*, 309–320.

Ross, A.J., Ruiz-Perez, V., Wang, Y., Hagan, D.M., Scherer, S., Lynch, S.A., Lindsay, S., Custard, E., Belloni, E., Wilson, D.I. et al. (1998). A homeobox gene, HLXB9, is the major locus for dominantly inherited sacral agenesis. Nat. Genet. *20*, 358–361.

Saha, M.S., Miles, R.R., and Grainger, R.M. (1997). Dorsal–ventral patterning during neural induction in Xenopus: assessment of spinal cord regionalization with xHB9, a marker for the motor neuron region. Dev. Biol. *187*, 209–223.

Schaeren-Wiemers, N., and Gerfin-Moser, A. (1993). A single protocol to detect trancripts of various types and expression levels in neural tissue and cultured cells: in situ hybridization using digoxigenin-labelled cRNA probes. Histochemistry *100*, 431–440.

Sharma, K., Sheng, H.Z., Lettieri, K., Li, H., Karavanov, A., Potter, S., Westphal, H., and Pfaff, S.L. (1998). LIM homeodomain factors Lhx3 and Lhx4 assign subtype identities for motor neurons. Cell *95*, 817–828.

Sockanathan, S., and Jessell, T.M. (1998). Motor neuron–derived retinoid signals determine the number and subtype identity of motor neurons in the developing spinal cord. Cell *94*, 503–514.

Tanabe, Y., and Jessell, T.M. (1996). Diversity and pattern in the developing spinal cord. Science *274*, 1115–1123.

Tanabe, Y., William, C., and Jessell, T.M. (1998). Specification of motor neuron identity by the MNR2 homeodomain protein. Cell *95*, 67–80.

Tosney, K.W., and Landmesser, L.T. (1985). Development of the

major pathways for neurite outgrowth in the chick hindlimb. Dev. Biol. *109*, 193–214.

Tsuchida, T., Ensini, M., Morton, S.B., Baldassare, M., Edlund, T., Jessell, T.M., and Pfaff, S.L. (1994). Topographic organization of embryonic motor neurons defined by expression of LIM homeobox genes. Cell *79*, 957–970.

Westendorf, J.M., Rao, P.N., and Gerace, L. (1994). Cloning of cDNAs for M-phase phosphoproteins recognized by the MPM2 monoclonal antibody and determination of the phosphorylated epitope. Proc. Natl. Acad. Sci. USA *91*, 714–718.

Wetts, R., Phelps, P.E., and Vaughn, J.E. (1995). Transient and continuous expression of NADPH diaphorase in different neuronal populations of developing rat spinal cord. Dev. Dyn. *202*, 215–228.

Zhao, D., McCaffery, P., Ivins, K.J., Neve, R.L., Hogan, P., Chin, W.W., and Dräger, U.C. (1996). Molecular identification of a major retinoic-acid-synthesizing enzyme, a retinaldehyde-specific dehydrogenase. Eur. J. Biochem. *240*, 15–22.